Electronic Supplementary Material (ESI) for Journal of Materials Chemistry A.

Organo-metal halide perovskite-based solar cells with CuSCN as inorganic hole selective contact

Sudam Chavhan,[a] Oscar Miguel,[a] Hans-Jurgen Grande,[a] Victoria Gonzalez-Pedro,[b] Rafael S. Sánchez,[b] Eva M. Barea,[b] Iván Mora-Seró[b],* and Ramón Tena-Zaera[a],*

[a]Energy Division, IK4-CIDETEC, Parque Tecnológico de San Sebastián, Paseo Miramón 196, Donostia-San Sebastián, 20009, Spain.

[b] Photovoltaic and Optoelectronic Devices Group, Department de Física, Universitat Jaume I, 12071 Castelló, Spain.

Supplementary information

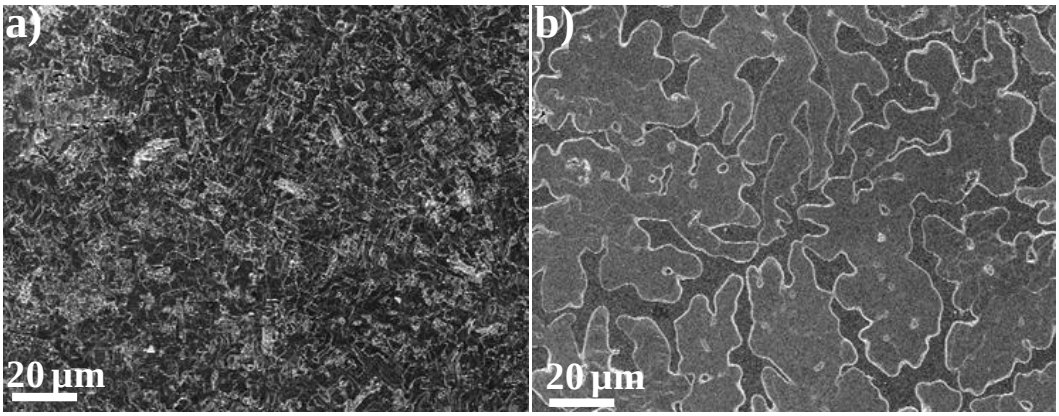

Figure S1 *: Top view FE-SEM micrographs of FTO/TiO_{2sp}/$CH_3NH_3PbI_{3-x}Cl_x$ samples obtained from solutions containing CH_3NH_3I synthesized by different routes: a and b. Both films were annealed at 110 ^oC for 3 hours.*

Synthetic routes used to obtain CH_3NH_3I:

a) Methyl ammonium iodide (CH_3NH_3I) was synthesized in accordance with reported method [1]. Briefly, in 30 ml methylamine (40 % in methanol, TCI), 32 ml hydroiodic acid (57 % in water, Aldrich) was added at 0 ºC in the ice bath and stirred continuously for 2 hours. Excess solvent was removed by rotary evaporator at 50 ºC, and obtained white powder was cleaned three times using diethyl ether. Finally, the product was dried at 60 ºC under vacuum for 24 hours.

b) Methyly ammonium iodide (CH_3NH_3I) was synthesized in accordance with the reported method in the reference 2. Briefly, 24 ml methylamine (33 wt % in ethanol) , 10 ml hydroiodic acid (57 wt % in water), and excess 100 ml absolute ethanol were added at room temperature under N_2 atmosphere and crystallization of final compound was obtained by using a rotary evaporator at 50 ^oC and final product was dried at 60 ºC under vacuum for 24 hours.

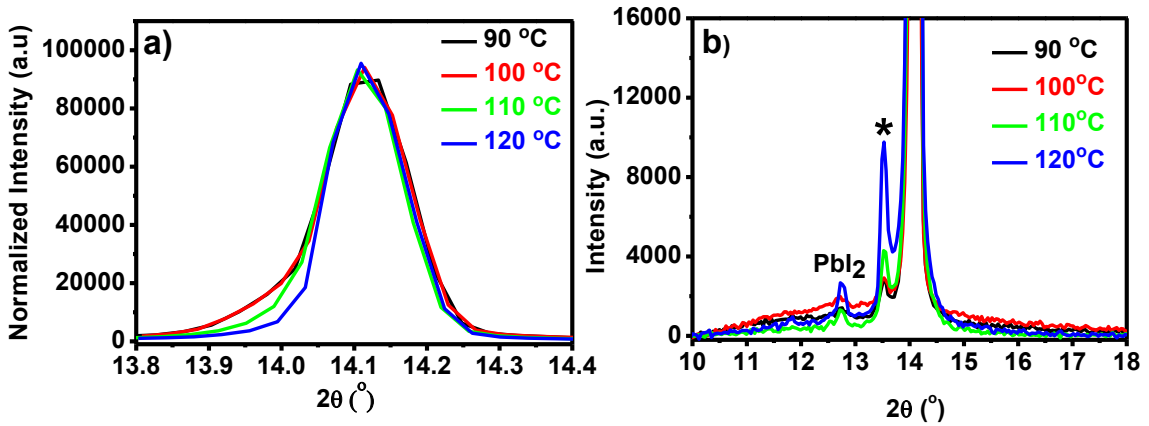

Figure S2: *a) Normalized (110) peak and b) partial view of the x-ray diffraction pattern of FTO/TiO_{2sp}/$CH_3NH_3PbI_{3-x}Cl_x$, annealed at different temperature for 3 hours in glove box. * Characteristic peak for the $CH_3NH_3PbI_{3-x}Cl_x$ films deposited from PbCl2.*

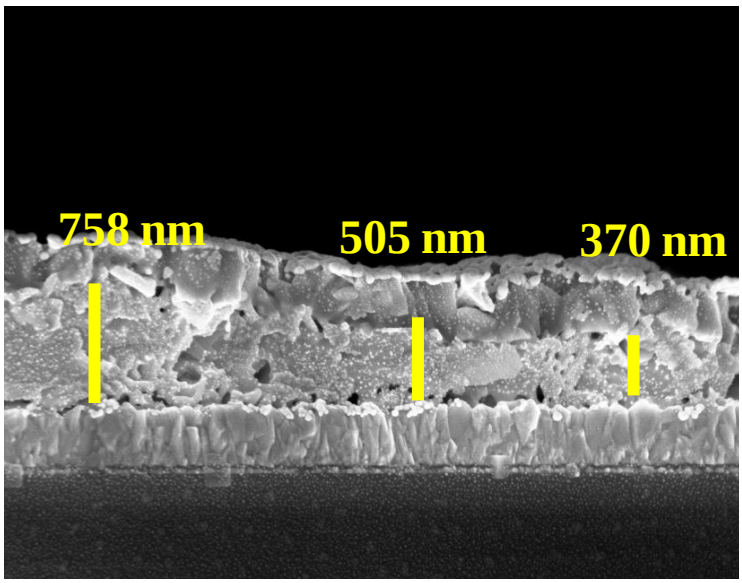

Figure S3*: Cross section FE-SEM micrograph of a complete solar cell (i.e. FTO/TiO_{2sp}/$CH_3NH_3PbI_{3-x}Cl_x$/CuSCN/Au), indicating the variation of $CH_3NH_3PbI_{3-x}Cl_x$, .layer thickness.*

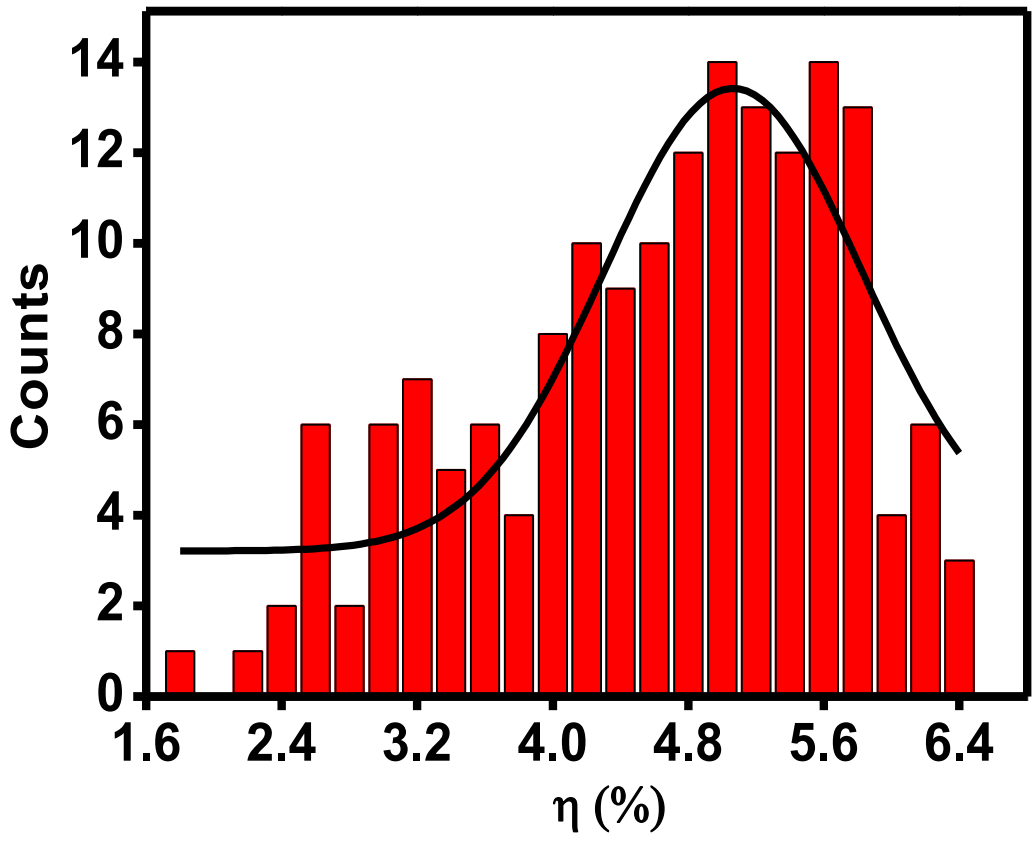

***Figure S4**: Power conversion efficiency of FTO/TiO_{2sp}/$CH_3NH_3PbI_{3-x}Cl_x$/CuSCN/Au solar cells (number of devices168).*

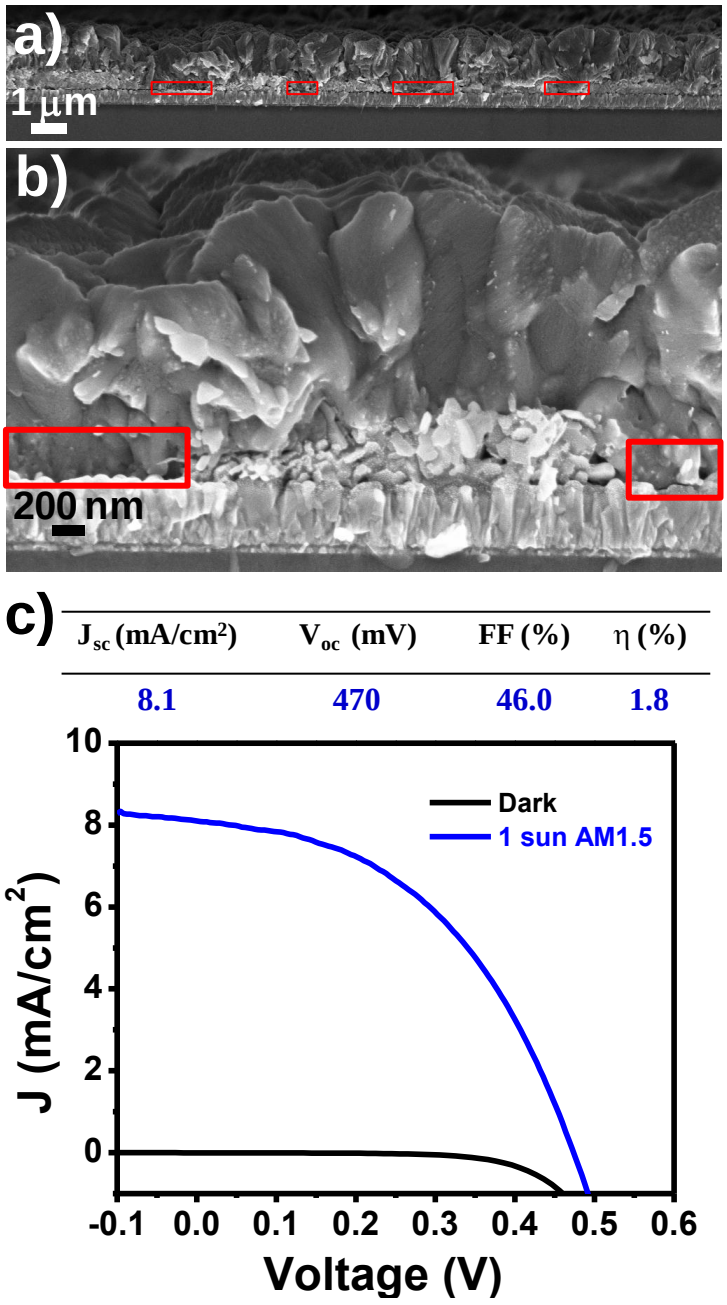

***Figure S5**: **a)** and **b)** FE-SEM micrographs of the cross section of a FTO/TiO_{2sp}/$CH_3NH_3PbI_3$/CuSCN heterostructure. The discontinuities of the $CH_3NH_3PbI_3$ film are highlighted (red rectangles). **c)** Photovoltaic parameters and current density-voltage characteristic of a FTO/TiO_{2sp}/$CH_3NH_3PbI_3$/CuSCN/Au solar cell.* $CH_3NH_3PbI_3$ was deposited by spinning 1 M PbI_2 and 1 M CH_3NH_3I DMF solutions and an ulterior thermal annealing at 100ºC (15 minutes).

Although the low quality of the $CH_3NH_3PbI_3$ films (preliminary results) does not allow a direct comparison between the photovoltaic parameters from $CH_3NH_3PbI_3$ *and* $CH_3NH_3PbI_{3-x}Cl_x$-based devices, the viability of using CuSCN as selective contact in $CH_3NH_3PbI_3$-based solar cells is pointed out.

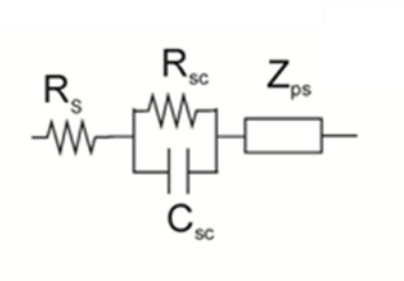

Figure S6: *Equivalent circuit for IS spectra fitting formed by a series resistance, Rs, and R-C Circuit denoted as sc (selective contact), related with the selective contacts (transport on CuSCN, Charge transfer at selective contact/ $CH_3NH_3PbI_{3-x}Cl_x$ interface), and the impedance due to bulk $CH_3NH_3PbI_{3-x}Cl_x$, Zps, formed by a Gerischer element or by Gerischer plus R-C in order to attain better fit.*

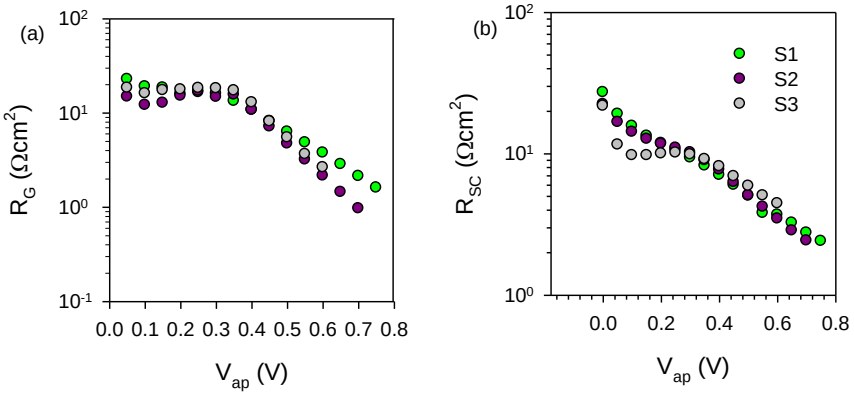

Figure S7: *Plot of recombination resistance (RG) (a) and the transport resistance associated with the selective contacts, (Rsc) (b) vs. the applied voltage.*

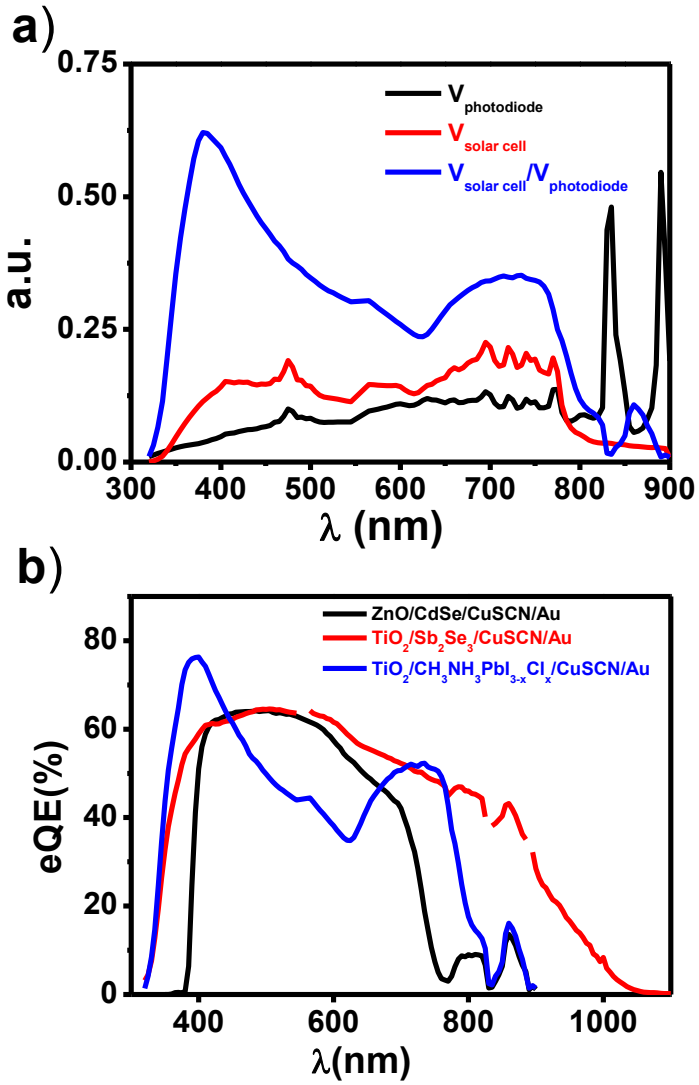

***Figure S8**: **a)** Spectral dependence of the signal amplitude for the reference Si photodiode, a FTO/TiO_{2sp}/$CH_3NH_3PbI_{3-x}Cl_x$/CuSCN/Au solar cell and ratio between both amplitudes. It is noted that each curve has been corrected by a constant factor in order to make possible the direct comparison in the graph scale. **b)** eQE of different solar cells characterized in the same spectral response set-up.*

Taking into account that the eQE of the reference Si photodiode is almost constant in the 400-1000 nm wavelength range, two strong peaks occurring at ~ 835 and ~ 890 nm in the emission spectra of the lamp can be concluded. The presence of these peaks in the signal from the reference Si photodiode results in two artifacts (~ 815 and ~ 860 nm) in the estimated eQE. However, the signal amplitude for the FTO/TiO_{2sp}/$CH_3NH_3PbI_{3-x}Cl_x$/CuSCN/Au solar cell is negligible for wavelengths longer than 800 nm, indicating no photon to electron conversion (i.e. no quantum efficiency) in this wavelength range. Furthermore, Figure S8b shows the eQE spectra estimated for solar cells based on semiconductor sensitizers (CdSe [3], $CH_3NH_3PbI_{3-x}Cl_x$, Sb_2Se_3 [4]) with different bandgaps. Irrespectively of the sensitizer, the artifacts occurring at ~ 815 and ~ 860 nm can be detected for all solar cells. However, the valley-like feature occurring around 600 nm is only detected for the perovskite-based device, pointing out a particular phenomena in this kind of solar cells. Further explanations on this phenomenon can be found in the paper.

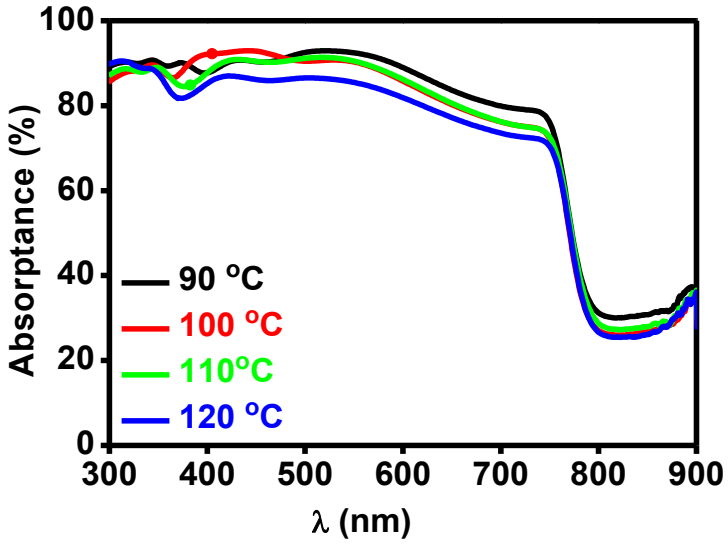

***Figure S9**: Absorptance spectra of FTO/TiO_{2sp}/$CH_3NH_3PbI_{3-x}Cl_x$ films annealed at different temperature for 3 hours.*

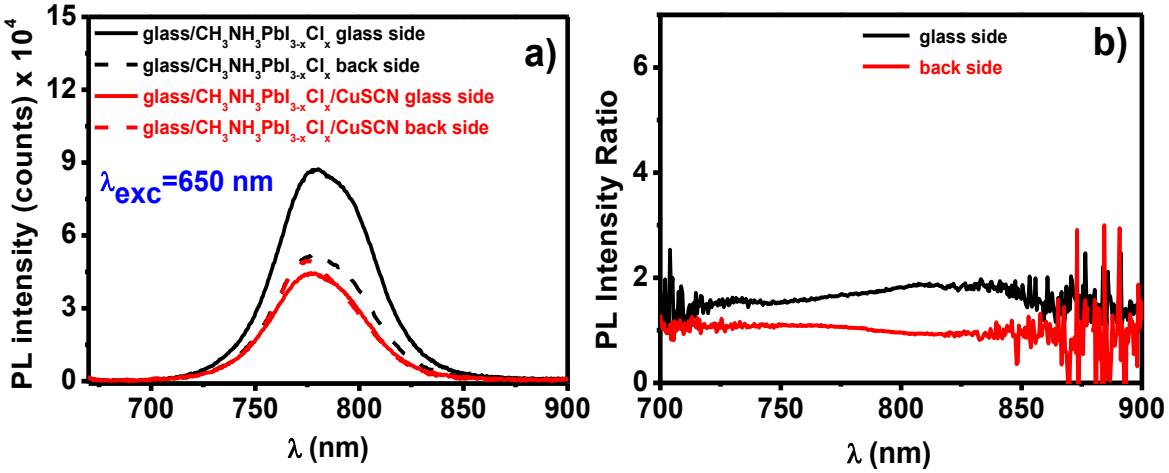

***Figure S10**: a) Photoluminescence spectra of glass/$CH_3NH_3PbI_{3-x}Cl_x$ films and glass/$CH_3NH_3PbI_{3-x}Cl_x$/CuSCN samples, b) ratio of photoluminescence yield between glass/ $CH_3NH_3PbI_{3-x}Cl_x$ and glass/ $CH_3NH_3PbI_{3-x}Cl_x$/CuSCN for the different excitation configurations.*

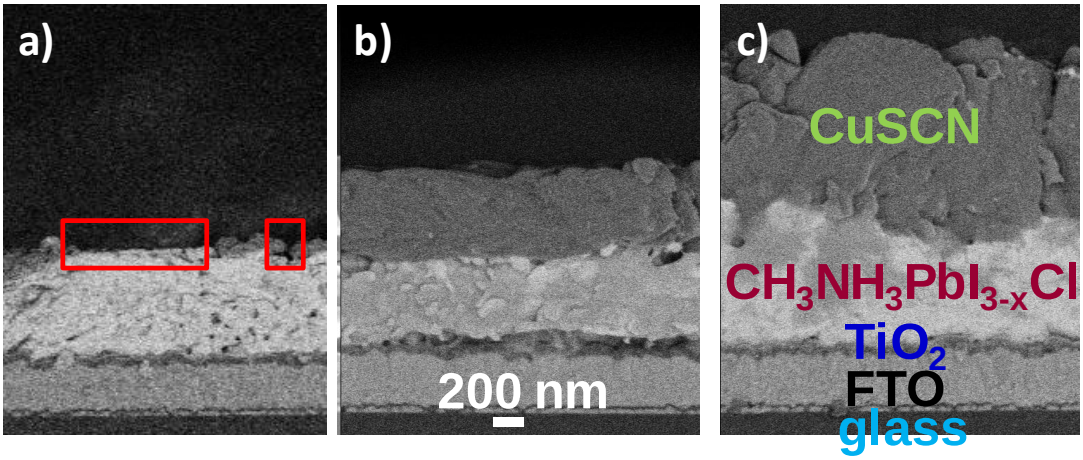

d)

CuSCN thickness (nm)	J_{sc} (mA/cm^2)	V_{oc} (mV)	FF (%)	η (%)
< 100*	13.2	590	50.4	3.9
~ 300	14.1	613	57.9	5.0
~ 500	14.3	591	60.6	5.1
~ 1000	14.0	646	55.8	5.2

** The CuSCN does not form a continuous film.*

***Figure S11**: FESEM micrographs -from the backscattered electron detector- of the cross of FTO/TiO_{2sp}/$CH_3NH_3PbI_3$/CuSCN heterostructures with different CuSCN thicknesses: a) < 100 nm, b) ~ 500 nm and c) ~ 1000 nm. d) The photovoltaic parameters of the corresponding solar cells.*

A relatively poor photovoltaic performance was detected for devices with non continuous CuSCN film. However, focusing on the solar cells with continuous CuSCN films, no significant effect of CuSCN thickness was detected. This finding suggests that hole transport in the CuSCN film does not seem to be a limiting factor, at least for thicknesses ≤ 1 μm.

References

1. J.-H. Im, C.-R. Lee, J.-W. Lee, S.-W. Park, N.-G. Park, *Nanoscale*, 2011, **3**, 4088.
2. M. M. Lee, J. Teuscher, T. Miyasaka, T. N. Murakami, H. J. Snaith, *Science*, 2012, **338**, 643.
3. I. Mora-Sero, S. Gimenez, F. Fabregat-Santiago, E. Azaceta, R. Tena-Zaera, J. Bisquert, *Phys. Chem. Chem. Phys*., 2011, **13**, 7131
4. T.T. Ngo, S. Chavhan, I. Kosta, O. Miguel, H-J. Grande, R. Tena-Zaera, *ACS Appl. Mater. Interfaces*, 2014, **6**, 2836.